PAGEOPH, Vol. 146, No. 1 (1996)

0033–4553/96/010021–21$1.50 + 0.20/0

A Determination of Source Properties of Large Intraplate Earthquakes in Alaska

HILARY J. FLETCHER[1] and DOUGLAS H. CHRISTENSEN[1]

Abstract—Historically, large and potentially hazardous earthquakes have occurred within the interior of Alaska. However, most have not been adequately studied using modern methods of waveform modeling. The 22 July 1937, 16 October 1947, and 7 April 1958 earthquakes are three of the largest events known to have occurred within central Alaska ($M_s = 7.3$, $M_s = 7.2$ and $M_s = 7.3$, respectively). We analyzed teleseismic body waves to gain information about the focal parameters of these events. In order to deconvolve the source time functions from teleseismic records, we first attempted to improve upon the published focal mechanisms for each event. Synthetic seismograms were computed for different source parameters, using the reflectivity method. A search was completed which compared the hand-digitized data with a suite of synthetic traces covering the complete parameter space of strike, dip, and slip direction. In this way, the focal mechanism showing the maximum correlation between the observed and calculated traces was found. Source time functions, i.e., the moment release as a function of time, were then deconvolved from teleseismic records for the three historical earthquakes, using the focal mechanisms which best fit the data. From these deconvolutions, we also recovered the depth of the events and their seismic moments. The earthquakes were all found to have a shallow foci, with depths of less than 10 km.

The 1937 earthquake occurred within a northeast-southwest band of seismicity termed the Salcha seismic zone (SSZ). We confirm the previously published focal mechanism, indicating strike-slip faulting, with one focal plane parallel to the SSZ which was interpreted as the fault plane. Assuming a unilateral fault model and a reasonable rupture velocity of between 2 and 3 km/s, the 21 second rupture duration for this event indicates that all of the 65 km long SSZ may have ruptured during this event. The 1947 event, located to the south of the northwest-southeast trending Fairbanks seismic zone, was found to have a duration of about 11 seconds, thus indicating a rupture length of up to 30 km. The rupture duration of the 1958 earthquake, which occurred near the town of Huslia, approximately 400 km ENE of Fairbanks, was found to be about 9 seconds. This gives a rupture length consistent with the observed damage, an area of 16 km by 64 km.

Key words: Intraplate seismicity, historical earthquakes, deconvolution, source-time function.

Introduction

Large ($M_s > 7$) intraplate earthquakes occur infrequently and irregularly. Given the potential hazards associated with such events, it is important to gain as much information as possible about these rare events. We have performed detailed analyses, including deconvolving source time functions from teleseismic body wave traces, for the three most recent $M_s > 7$ earthquakes in interior Alaska, occurring

[1] Geophysical Institute, University of Alaska Fairbanks, Fairbanks, AK 99775-7320, U.S.A.

in July 1937, $M_s = 7.3$, October 1947, $M_s = 7.2$, and April 1958, $M_s = 7.3$ (magnitudes from ABE, 1981). The 1937 and 1947 earthquakes both occurred in central Alaska, an area where, despite the substantial intraplate activity, little is known about the causative processes. The 1958 earthquake occurred in western Alaska, an area of low seismicity, so again little is known about the tectonic processes active in this area. Thus, studies of these large historical earthquakes provide a unique opportunity to examine the seismicity and seismotectonics of central and western Alaska.

Tectonic Setting

The majority of earthquakes in Alaska, excluding those in west central Alaska, appear to result from the interaction of the Pacific and North American lithospheric plates (DAVIES, 1983; ESTABROOK *et al.*, 1988; PAGE *et al.*, 1991). The northwest motion of the Pacific plate relative to the North American plate is accommodated by dextral transcurrent faulting in southeast Alaska, and by underthrusting and

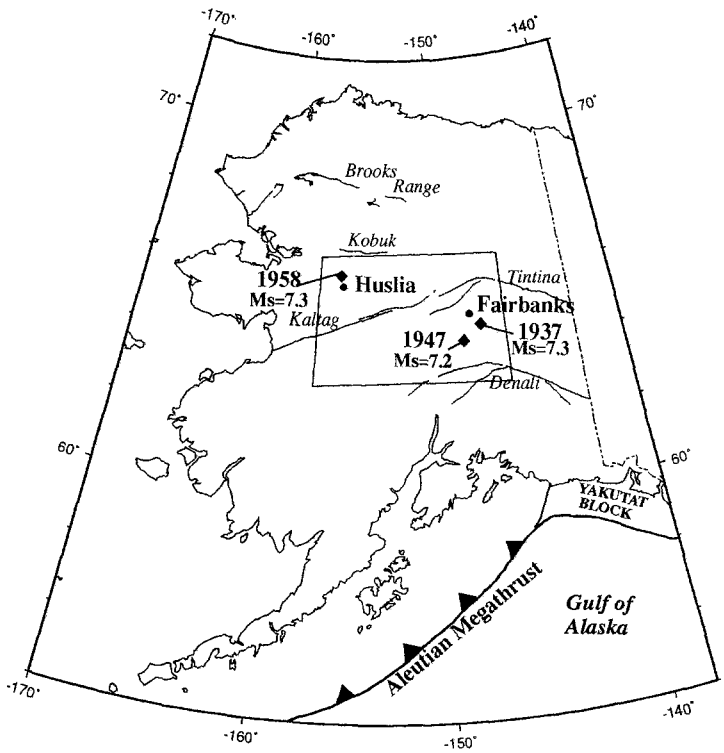

Figure 1
Map of Alaska showing the epicenters of the earthquakes in this study. Also shown are the traces of major fault systems. The outlined area is enlarged in Figure 2.

subduction of the Pacific plate beneath the North American plate along the Aleutian trench (PAGE *et al.*, 1991). Complexity is added to this simple model in the transitional area between transcurrent and convergent segments of the plate boundary. Here the Yakutat terrane, still part of the Pacific plate, is docking against the continent and resisting subduction. The horizontal compressional stress from this collision is transmitted inland across the eastern half of the state, resulting in a broad zone of deformation and seismicity (PAGE *et al.*, 1991), and seaward into the Pacific plate (LAHR *et al.*, 1988). In western Alaska, and on the Seward Peninsula, the seismicity and recent tectonism reflect regional extension (BISWAS *et al.*, 1986).

Some of the major tectonic features in the vicinity of the three earthquakes in this study are shown in Figure 1. Both the 1937 and 1947 earthquakes lie between two large dextral fault systems, the Denali fault to the south and the Tintina fault to the north. Estimates of Holocene slip rates on the Denali fault are between 8 and 14 mm/yr (SIEH, 1981). The Tintina fault runs parallel to the Denali fault, about 250 km to the north. Geologic evidence indicates that the current average rate of slip on the Tintina fault system is 5 mm/yr or lower, less than that on the Denali system (PAGE *et al.*, 1995). The 1958 Huslia earthquake occurred in the Koyukuk Basin south of the Brooks range. The main tectonic features in the area include the Kaltag right-lateral strike-slip fault to the south, and the Kobuk right-lateral strike-slip fault and the Brooks Range to the north.

Seismicity

The historical record of seismicity in central and west central Alaska, which is derived mainly from teleseismic recordings of moderate and large earthquakes, includes eleven shocks of $M_s > 6.0$ before 1960, all of which are located between latitudes 63.0°N and 66.5°N, and between longitudes 147.0°W and 158.0°W (illustrated in Figure 2, which shows all earthquakes through 1994 with $M_s > 6.0$ that have occurred in the area). Four of these have a magnitude of 7.2 or greater, three in the vicinity of Fairbanks (in 1904, 1937, and 1947), and one in west central Alaska (in 1958). We will study the three most recent of these earthquakes; the 1904 earthquake has too few usable recordings, and may in fact be substantially mislocated.

Seismicity in interior Alaska does not fall on individual through-going major faults, but is distributed over a broad area and possibly extends over several tectonic regimes. These intraplate events are most likely related to plate motions to the south, but not in a simple manner. Regions of tensional as well as compressional stresses may be expected, representing different modes of releasing the accumulated energy from plate motions. Crustal earthquakes pervade practically the entire state, with a prominent belt of diffuse activity extending north into

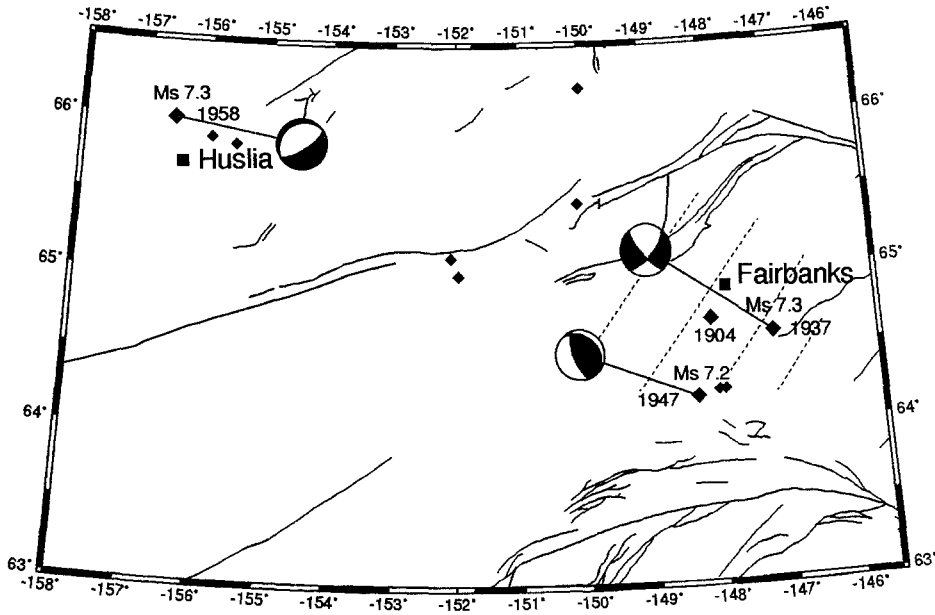

Figure 2

Map of western and central Alaska showing epicenters of all earthquakes through 1994 with $M_s > 6$. Small diamonds mark earthquakes with $M_s < 7$. The three earthquakes in this study are shown along with their magnitude and year of occurrence and focal mechanism. Focal mechanisms are lower hemisphere projections with shaded areas representing compressional quadrants, from WICKENS and HODGSON (1967) for the 1937 and 1947 events, and from REISER (1990) for the 1958 event.

interior Alaska, although there are few obvious correlations between the spatial distribution of earthquakes and the surface traces of major faults. Correlations have been suggested between shock of M 3 and several mapped faults in the interior of Alaska, such as the Tintina (ESTABROOK *et al.*, 1988) and the Kobuk (GEDNEY and MARSHALL, 1981) faults. However, in many cases, uncertainty in the epicenters makes the correlation with a specific mapped fault trace tenuous. The northern boundary of earthquake activity is marked by the Brooks Range, and the western part of the North Slope appears to be essentially aseismic.

Recent seismicity in the Fairbanks area is broadly distributed, as determined from data recorded by the regional seismic network installed in late 1966, now run by the Alaska Earthquake Information Center, which is jointly operated by the Geophysical Institute at the University of Alaska Fairbanks and the U.S. Geological Survey. The overall pattern of epicenters displays a general NE-SW grain with several noteworthy clusters and trends. The distribution of earthquakes defines three distinct regions (see Figure 3), named the Salcha, Fairbanks, and Minto Flats seismic zones (BISWAS and TYTGAT, 1988).

The Salcha seismic zone (SSZ) is a well-defined seismic lineation approximately 60-km long and contains the epicenter of the July 1937, $M_s = 7.3$, earthquake. It is

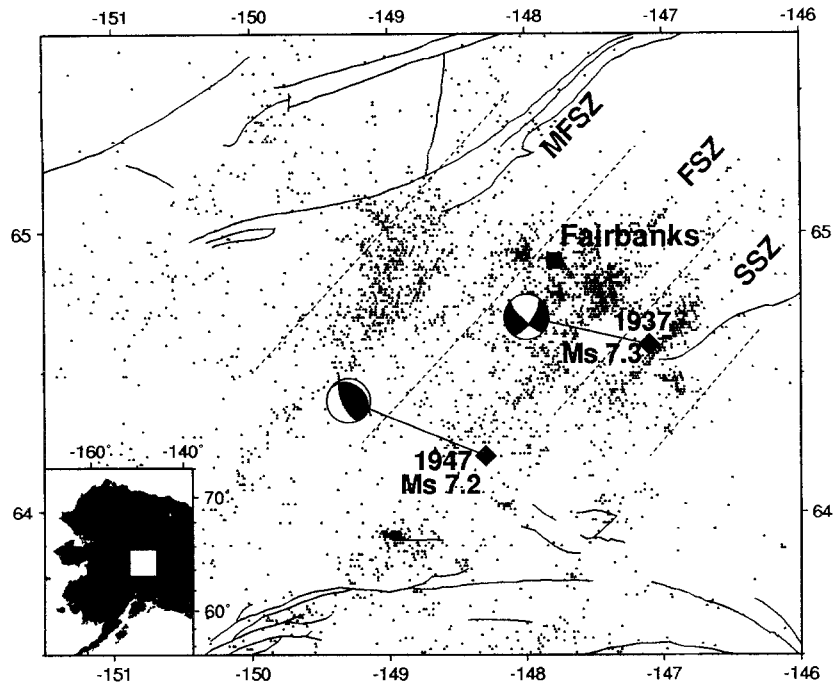

Figure 3
Epicentral plot of located earthquakes which occurred between 1988 and 1994 in central Alaska, $M < 5$. The source of the data is the earthquake catalog of the University of Alaska Fairbanks. The Minto Flats seismic zone (MFSZ), Fairbanks seismic zone (FSZ), and Salcha seismic zone (SSZ) are visible as northeast striking bands of seismicity.

thought that perhaps the large historical earthquakes and the associated recent seismicity mark an active fault zone, although no evidence of Quaternary displacement has yet been recognized (CLUFF *et al.*, 1974). Two earthquakes with $M_s = 6.25$ and 6.5 occurred in 1929 about 50 km further southwest along the same NE-SW trend, although the epicenters of these events are uncertain by several tens of kilometers. These two earthquakes lie in an area which shows a clustering of recent earthquakes, and it is not clear whether this cluster is a part of the SSZ, or rather related to the nearby 1947 earthquake.

The Fairbanks seismic zone, or FSZ (GEDNEY *et al.*, 1980), is an active region, in which earthquakes occur frequently. This zone was the site of three $M_s = 5.5$ to 5.9 earthquakes in 1967, which occurred within minutes of each other. These events were followed by a prominent aftershock sequence distributed over an area of approximately 15 km in diameter and extending to a maximum depth of 20 km (GEDNEY and BERG, 1969). Since 1967, five or six felt earthquakes per year have occurred in this zone, along with periodic surges of intense microearthquake activity which tend to last from a few days to a month and show spatial migration

(GEDNEY *et al.*, 1980). These swarms do not fall on a single simple feature, nor do they appear to line up with the larger scale NE-SW trend, rather they occur over a broad region, indicating that the tectonics in this area are complicated. The epicenter of the October 1947 event is located further south along the trend of the FSZ.

The Minto Flats seismic zone (MFSZ) is a diffuse region of seismicity. Some of the apparent scatter may be an artifact of weak geometry in the network of stations recording the earthquakes. However, lying along the axis of the diffuse seismic band is the Minto lineament, which has been mapped as a fault (PEWE *et al.*, 1966), although more recently it has been categorized as a geomorphic feature.

The 22 July 1937 Earthquake

The epicenter of the 1937, $M_s = 7.3$, earthquake (64.67°N, 146.58°W) is located in the center of the SSZ, a NE-SW trending zone of seismicity approximately 65 km long (Figure 3). A field survey was carried out shortly after the principal shock, which gave a location of roughly 64.4°N, 146.5°W from damage and felt reports (BRAMHALL, 1938). From the same field study, a felt area with a radius of 500 km from an origin near the city of Salcha is reported. This would correspond to a felt area of almost 800,000 km^2. The earthquake was preceded by a number of smaller local shocks (BRAMHALL, 1938), and followed by numerous aftershocks spanning several months (ADKINS, 1939). The epicenter of the main shock is located 98 km from College observatory (COL), the nearest seismic station.

The 16 October 1947 Earthquake

This central Alaskan earthquake with $M_s = 7.2$, located at the southern end of the FSZ (epicenter 64.2°N, 148.3°W; see Figure 3), was preceded by foreshocks and followed by numerous aftershocks including one on 20 October, 1947, that registered a magnitude of approximately $M_s = 6.8$. Following the main shock, a field study was undertaken, results of which were reported by ST. AMAND (1948). Based on these results, he concluded a location of 64.2°N, 149.0°W, and the investigation revealed Modified Mercalli intensities of at least VIII in the epicentral region, near the intersection of the Nenana and Tanana Valleys. ST. AMAND (1948) indicates a felt area slightly larger than that reported for the 1937 earthquake and reports that many people were of the opinion that the main shock in 1947 was of slightly greater strength than that of 1937.

The 7 April 1958 Earthquake

The $M_s = 7.3$ earthquake of 7 April, 1958 (epicenter 65.99°N, 156.55°W) was the largest of a series of shocks centered in an area near Huslia in the Koyukuk

Basin, south of the Brooks Range and north of the Kaltag fault, approximately 400 km ENE of Fairbanks (Figure 2). Two magnitude 6 aftershocks followed within a week of this event. A field report by DAVIS (1960) states that the main shock of the series registered a Modified Mercalli intensity V or more over an area in excess of 180,000 km^2, with a felt area of 640,000 km^2. From this report, the location was determined to be at 65.75°N, 155.75°W, and the most severe damage of the main shock occurred in a zone approximately 16-km wide by 64-km long trending northeast from Huslia (DAVIS, 1960).

Data

Data for this study were obtained from the National Earthquake Information Center (NEIC) archives, and by making requests to worldwide stations known to be in operation between 1937 and 1958. Problems with the data included: (1) a sparse data set, (2) unknown instrument parameters, (3) low signal-to-noise ratio for some stations, and (4) poor quality copies of the analog traces. The data used were recorded on Galitzin, Wenner, Benioff, Wiechert, and Wood-Anderson seismometers. The analog records were hand-digitized, and the quality of the resulting digitized traces was tested by superimposing them on the originals. Due to the poor

Table 1

Table of instrument parameters for all stations used in his study. To and Tg are the seismometer and galvanometer periods, h1 and h2 are the seismometer and galvanometer damping. Sources of this information are from POPPE (1979), *and from the individual station.*

Station	Component	Instrument	*To*	*Tg*	*h1*	*h2*	*Mag. at To*
PAS	E	Benioff	1.0	90.0	1.0	1.0	3000
	N	Benioff	1.0	90.0	1.0	1.0	3000
	Z	Benioff	1.0	90.0	1.0	1.0	3000
SJG	E	Wenner M2	9.65	13.7	0.69	1.0	1280
	N	Wenner M1	9.75	20.0	0.69	1.0	1000
TUC	E	Wood-And	7.8		0.8		457
	N	Wood-And	7.6		0.8		466
	Z	Benioff	1.0	77.0	1.0	0.34	30,000
LPB	Z	Galitzin	10.1	11.74	1.0	1.0	1300
ABU	E	Wiechert	10.0		0.45		170
	N	Wiechert	10.0		0.45		170
	Z	Wiechert	4.7		0.43		150
PUL	E	Galitzin	13.0	13.0	1.0	1.0	1100
	N	Galitzin	13.0	13.0	1.0	1.0	1100
	Z	Galitzin	12.2	13.1	1.0	1.0	700
DBN	E	Galitzin	25.0	25.0	1.0	1.0	310
	N	Galitzin	25.0	25.0	1.0	1.0	310
	Z	Galitzin	12.0	12.0	1.0	1.0	740
TIF	Z	Galitzin	12.0	12.3	1.0	1.0	1200

quality of much of the data, despite obtaining records from over 15 stations, we could analyze records from just four stations for the 1937 event, six stations for the 1947 event, and four stations for the 1958 event. The stations used were: Abuyama, Japan (ABU); De Bilt, Netherlands (DBN); La Paz, Bolivia (LPB); Pasadena, California (PAS); Pulkovo, Russia (PUL); San Juan, Puerto Rico (SJG); Tiflis, Georgia (TIF); and Tucson, Arizona (TUC). A complete list of stations and instrument parameters is given in Table 1. From these instrument parameters we calculate the response of the Galitzin from MACELWANE and SOHON (1932, p. 94). The Wood-Anderson response is calculated from SEIDL (1980) and we follow the method of ESTABROOK and BOYD (1992) in determining the response for a simple mechanical instrument.

Test of Published Source Parameters

In order to test the reliability of published focal mechanisms for the three events, we used a method originally proposed by BEISSER and KIND (1988), developed by BEISSER *et al.* (1990) for use with sparse data sets, and further tested and modified by BEISSER *et al.* (1994). Synthetic seismograms were calculated in a ten degree grid for every source orientation, using the reflectivity method as described in MÜLLER (1985). The complete *P*-, *SV*-, and *SH*-wave groups were computed, including all depth and mantle phases. The crustal model in the vicinity of the earthquakes was taken from BEAUDOIN *et al.* (1992). Below the receivers a simple *P*-wave velocity model of 6 km/s from 0–30 km depth and 7 km/s from 30–40 km was used, as we did not know the crustal structure under the stations. *S*-wave velocity was based on the *P*-wave velocity and a Poisson's ratio of 0.25. For depths greater than 40 km we used the PREM (DZIEWONSKI and ANDERSON, 1981). A systematic grid search of the complete parameter space of strike, dip, and slip direction was completed to find the best fitting focal mechanism. The source used in the original code is a dislocation point source with a time function derived from the ramp moment function according to BRUESTLE and MÜLLER (1983). This was modified to allow a trapezoid time function, consistent with our experience of the method of moment release in earthquakes of this size. We cross-correlated the synthetic traces with the data, scaling the synthetic traces such that the maximum amplitude was equal to that of the data. A correlation coefficient was calculated to describe the fit for each synthetic, i.e., for each set of focal parameters. If the correlation was negative it was set equal to zero. A matrix of strike, dip, slip, and correlation was obtained for each component of a station. The correlation matrices for all components were multiplied together for each station, thus giving each component an equal weighting, and the results from different stations were combined by multiplying the matrices of each station. Each component and station provides certain constraints on the solution, which, when combined, provide an overall best solution.

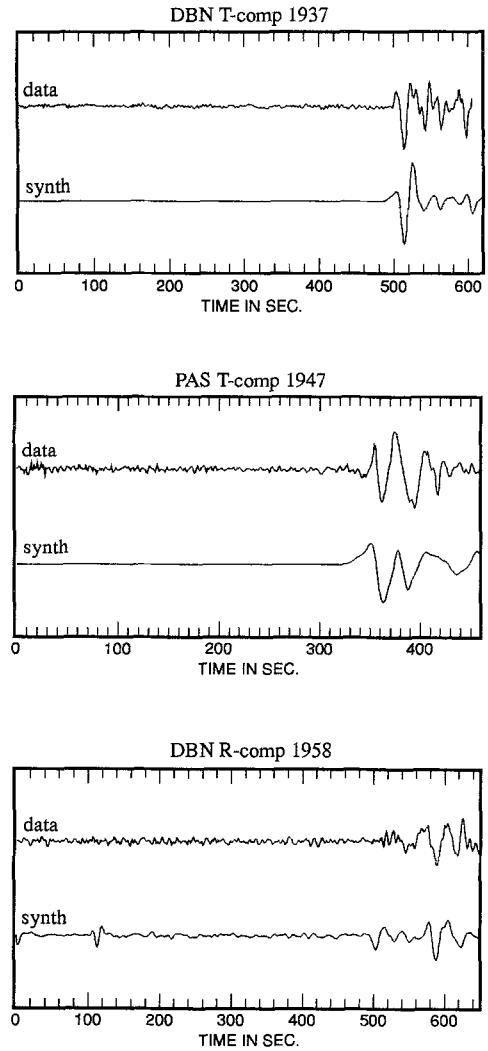

Figure 4

Examples of the match between data and synthetics computed with source orientations of strike = 40°, dip = 70°, slip = 340° for the 1937 event, strike = 160°, dip = 70°, slip = 100° for the 1947 event, and strike = 60°, dip = 70°, slip = 270° for the 1958 event. The synthetics were calculated using a trapezoid source time function with a duration of 20, 11, and 10 seconds for the three earthquakes, respectively.

Results

For the 1937 Salcha event we used seven components: ABU, 2 components; DBN, 3 components; TUC, 2 components. Six traces were used for the 1947 event; DBN, 2 components; PAS, 2 components; SJG, 2 components. Only five traces were selected for the 1958 Huslia event: DBN, 3 components; ABU, 1 component; PAS, 1 component. Examples of the data, and the fit to the synthetics, can be seen

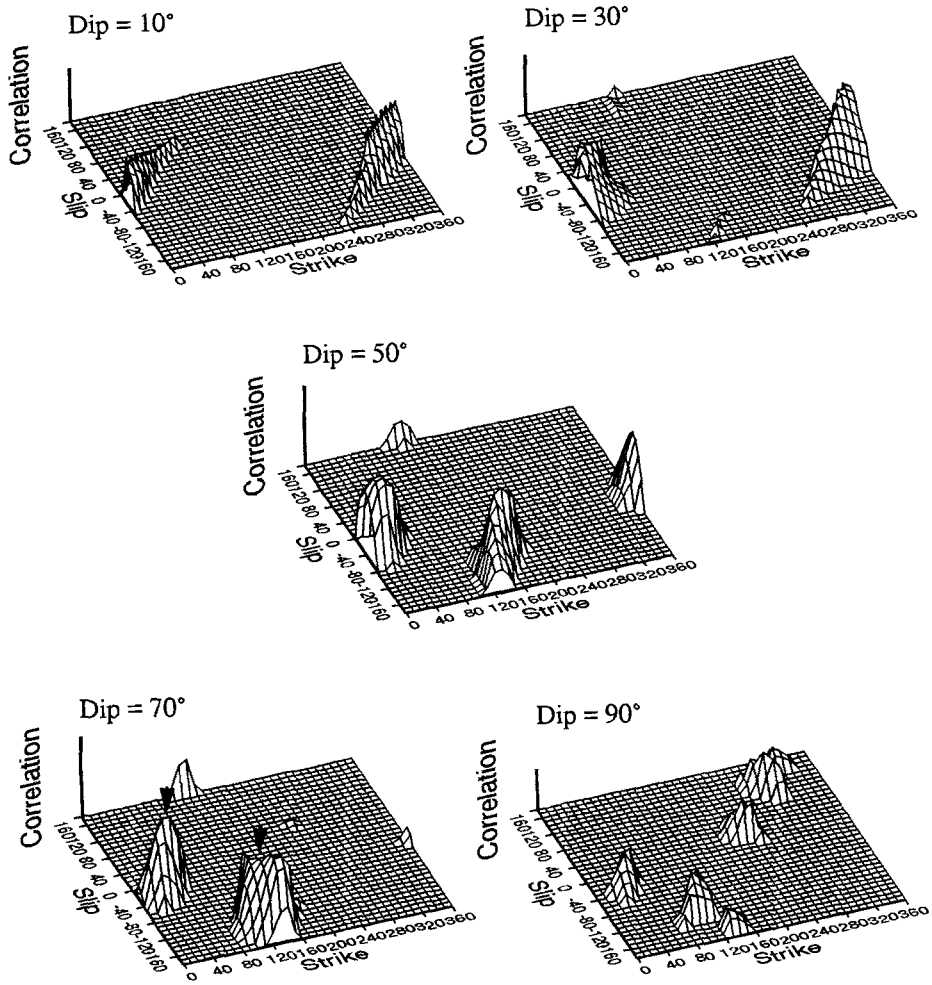

Figure 5
Correlation matrices for the 1937 Salcha earthquake. This is the result of the multiplication of the correlation matrices of stations ABU, DBN, and TUC. The grid spacing is 10° for the strike and slip angle. Each plot is for a constant dip, and not all dips are shown. The arrows indicate the nodal planes of the previously published focal mechanism.

in Figure 4. The results are best illustrated by plotting the correlation matrix: each plot in Figures 5 and 6, for the 1937 and 1958 earthquakes, shows the correlation of the digitized data with the calculated synthetics as a function of strike and slip for a constant dip. The best solution is represented by the highest peak which, for a unique solution, should be at least 20% higher than the peak of any other solution (BEISSER *et al.*, 1994). Our results confirm that the most recently published focal mechanisms for both the 1937 event, strike = 35.2°, dip = 66.8°, slip = 341.9° (WICKENS and HODGSON, 1967), and for the 1958 event, strike = 54.0°,

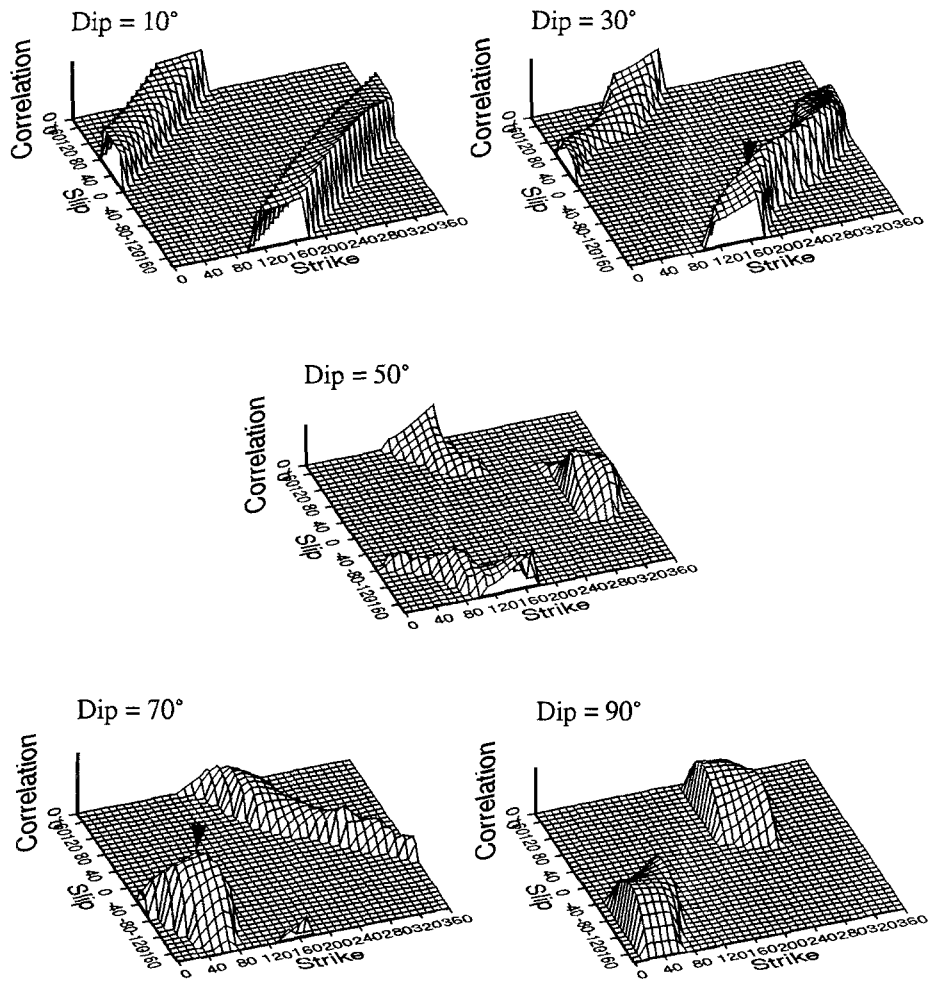

Figure 6
Correlation matrices for the 1958 Huslia earthquake. This is the result of the multiplication of the correlation matrices of stations ABU, DBN, and PUL. The grid spacing is 10° for the strike and slip angle. Each plot is for a constant dip, and not all dips are shown. The arrows indicate the nodal planes of the previously published focal mechanism.

dip = 70.0°, slip = 270.0° (REISER, 1990), shown in Figure 2, are possible and indeed likely. However, due to the poor data, a unique focal mechanism can only be found for the 1937 event. The correlation data for the 1937 earthquake give two 'maxima' at a dip of 70°, illustrated in Figure 5 as two broad peaks, which correlate with the two nodal planes of the published focal mechanism. The width of the peaks determines the quality of the solution, and these results reveal that the strike, dip and slip can vary over $\pm 20°$ and still produce the same fit to the data. The correlation results for the 1958 earthquake show one 'maximum', at a dip of 70°,

corresponding to the focal plane of the published focal mechanism (Figure 6). However, the other nodal plane has no peak associated with it, indicating that this plane is less well constrained. The overall result for this earthquake is not as constrained as that for the 1937 event, illustrated by the presence of other regions of high correlation.

The published thrust mechanism for the 1947 event is strike = 155.7°, dip = 67.2°, slip = 102.2° (WICKENS and HODGSON, 1967). We had hoped to be able to determine an improved result, however, the correlation results do not constrain any focal parameters. Using the first motion data from our traces combined with the first motion information from the International Seismological Summary (1947), and in HODGSON and MILNE (1951), we attempted to find a well-constrained focal mechanism for this event, but we could not improve upon the previously published result.

P-wave Deconvolution and Rupture Process

The earthquakes were modeled using seismograms recorded teleseismically, where there are fewer complications in the P and S waves due to earth structure. In this distance range the elastic earth response can be adequately modeled using geometric ray theory, i.e., there is no significant distortion of the waveshape.

Synthetic seismograms for body waves at teleseismic distances can be constructed as $s(t) = i(t)*g(t)*m(t)$, where * denotes convolution, $s(t)$ is the seismogram, $i(t)$ is the instrument impulse response, $g(t)$ contains the source geometry (including P, pP, sP) and the earth's impulse response, and $m(t)$ is the source time function. Assuming that the average fault geometry is known, $m(t)$ is then obtained by inverting the convolution operation. The single-station deconvolution method we used is described in RUFF and KANAMORI (1983), who use a time domain method for the inversion; the source time functions are deconvolved with a time interval of 0.8 seconds.

The depth determination of intermediate-size ($M_s = 6.5$ to 7.5), shallow (≤ 60 km) earthquakes is problematic due to indistinct depth phases; thus body wave modeling is necessary. However, using body wave modeling techniques, the depth is poorly resolved due to the trade-off between depth and source function. We determined the range of acceptable depths following the observations of CHRISTENSEN and RUFF (1985), who demonstrated that incorrect depth assumptions cause spurious pulses in the source time function. These complications can easily be recognized in the deconvolved source time functions of earthquakes, and used to constrain the depth extent. Source time functions were thus computed for a range of increasing depths and the best depth range was determined from the consistency and simplicity of the source time functions.

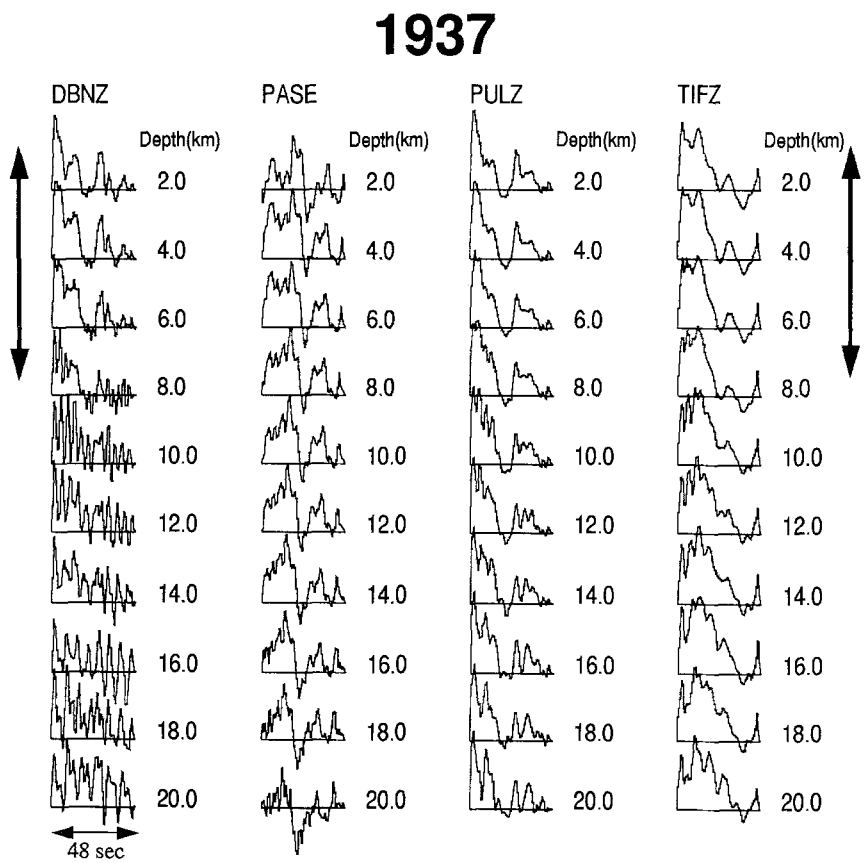

Figure 7
Deconvolved source time functions at different depths from seismograms of the 1937 earthquake. The arrow marks the depth extent of 'simple' source time functions.

Results

Figures 7, 8, and 9 illustrate our method of determining the acceptable depth ranges of the earthquakes. For each earthquake, source time functions were deconvolved from all traces for a range of increasing depths. In order to be used in the deconvolutions, the data needed to show clear *P*-wave arrivals. For the 1937 earthquake we used the vertical component of stations DBN, PUL, TIF, and a horizontal component of the station PAS. Three good quality vertical records were found for the 1947 event at stations DBN, LPB, and PAS, and two horizontal components at stations SJG and TUC. For the 1958 earthquake we used vertical component records from stations ABU, DBN, PAS, and PUL. Following the technique of CHRISTENSEN and RUFF (1985), the depth range for which the source time functions are the most simple is believed to be the correct depth range. The

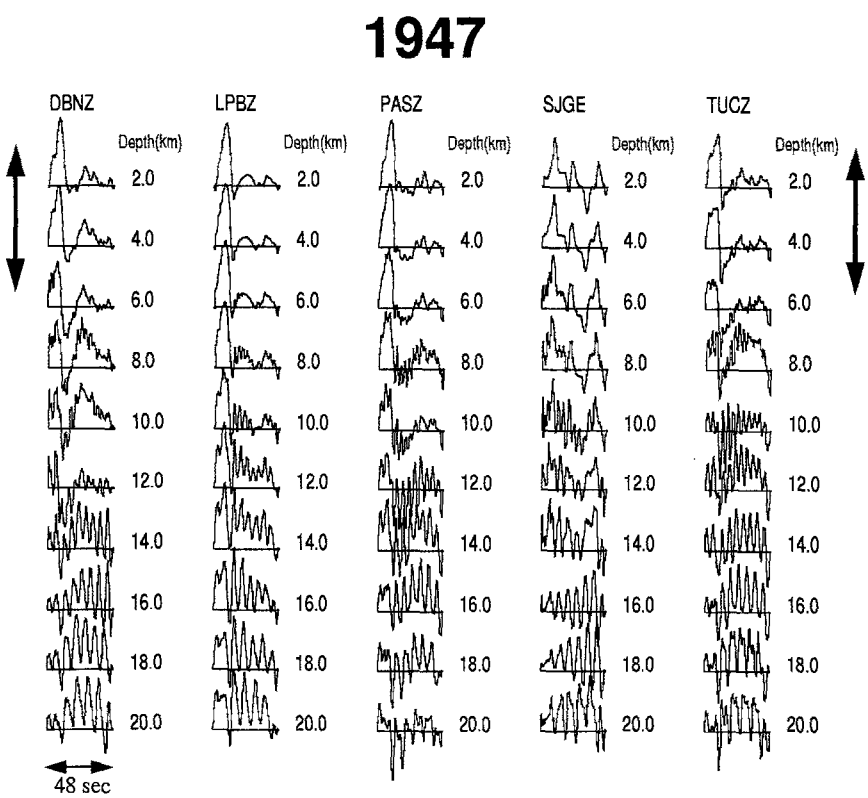

Figure 8
Deconvolved source time functions at different depths from seismograms of the 1947 earthquake. The arrow marks the maximum depth extent of 'simple' source time functions.

arrows indicate the depth extent of the 'simple' source time functions. We deduced depth ranges of 2 km to 8 km for the 1937 event, 2 km to 6 km for the 1947 event, and 2 km to 8 km for the 1958 event. We do not believe these depths can be resolved with errors better than ± 4 km, and thus for the final deconvolutions we assume a rupture extent from 1–10 km in all cases.

Source time functions were once more deconvolved, this time using a distributed source Green's function, with a depth range of 1–10 km. These final results (Figures 10, 11 and 12) gave an average rupture time of 21 ± 3 seconds for the 1937 event, 11 ± 1 seconds for the 1947 event and 9 ± 2 seconds for the 1958 event. The source time functions of the 1937 event (Figure 10) are more complex than the simple single pulses seen in the source time function of the 1947 and 1958 events (Figures 11 and 12). The earthquakes were found to have seismic moments of $0.6 \pm 0.2 \times 10^{27}$ dyne.cm, $0.5 \pm 0.2 \times 10^{27}$ dyne.cm, and $0.2 \pm 0.1 \times 10^{27}$ dyne.cm for the 1937, 1947, and 1958 events, respectively. From these results, moment magnitudes were calculated for the three events: $M_w = 7.2$ for the 1937 earthquake, $M_w = 7.1$ for the 1947 earthquake, and $M_w = 6.8$ for the 1958 earthquake.

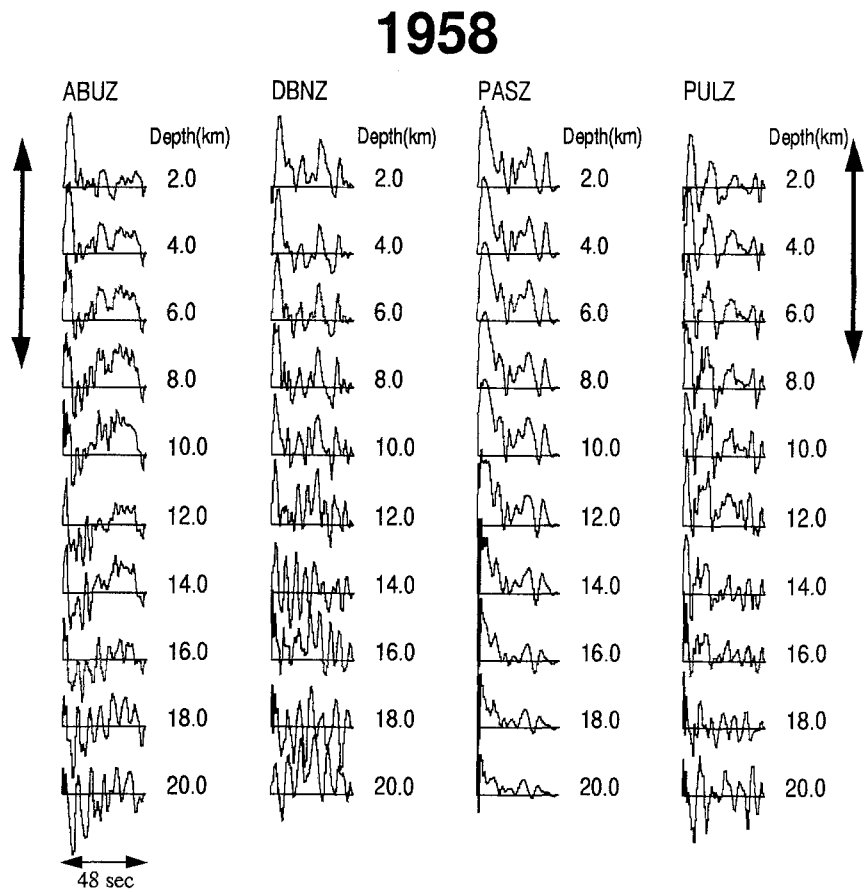

Figure 9
Deconvolved source time functions at different depths from seismograms of the 1958 earthquake. The arrow marks the maximum depth extent of 'simple' source time functions.

Discussion and Conclusions

The 1937 and 1947 earthquakes are located between the Denali and Tintina fault systems in east central Alaska (Figure 3). Gravity, aeromagnetic, seismic and geological data from this area indicate numerous northeast to north-northeast striking, steeply-dipping faults, exhibiting sinistral slip (RAINER NEWBERRY, personal communication; GRISCOM, 1976; NOKLEBERG *et al.*, 1992). PAGE *et al.* (1989, 1995) proposed a tectonic model for this area of central Alaska. They suggest that this set of faults divides the crust into large elongated blocks, which rotate clockwise as a result of the northerly compression, within a broad dextral shear zone between the Denali and Tintina fault systems. This model allows for a

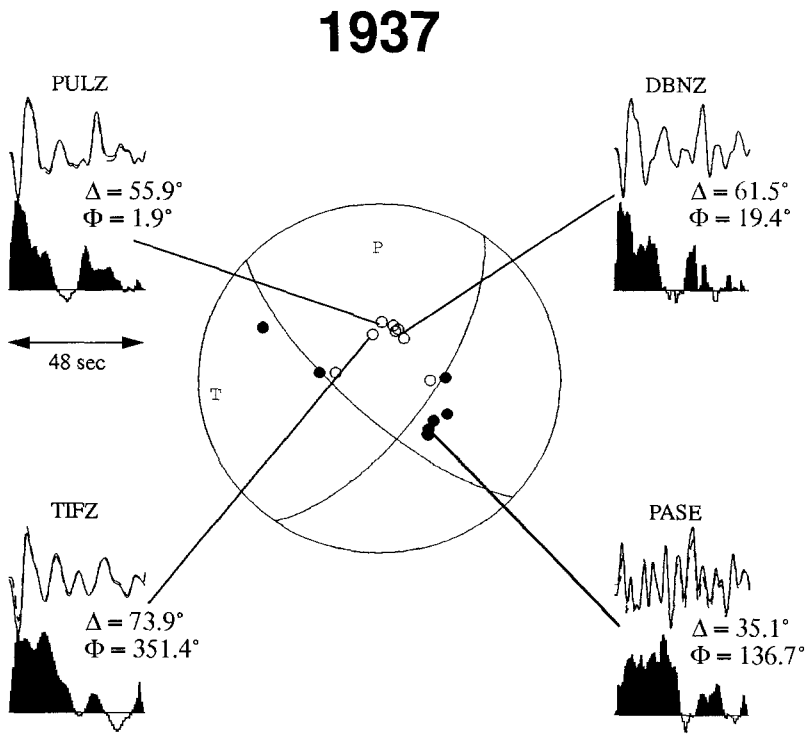

Figure 10
Focal mechanism of the 1937 earthquake used in the deconvolutions, from WICKENS and HODGSON (1967). The first motions are from the ISS bulletins using only stations where polarities are verified. Deconvolved source time functions, using a distributed source Green's function, are shown for stations PUL, DBN, TIF, and PAS. The data are shown by the solid traces, and the dashed traces are synthetics produced from the source time functions. Δ is the station-epicenter distance, and Φ is the station azimuth.

variety of tensional and compressional stresses within the area. The 1937 earthquake, occurring within a NE-SW band of seismicity termed the Salcha seismic zone, or SSZ (BISWAS and TYTGAT, 1988), has a focal mechanism indicating strike-slip faulting, with one focal plane parallel to the SSZ which was interpreted as the fault plane. Assuming a unilateral fault model and a reasonable rupture velocity of 2 to 3 km/s, the 21 second rupture duration for this event results in a unilateral rupture length of 40–60 km. However, the basic assumption of a simple unilateral model may not be accurate. The source time functions for this event are longer and more complex than those associated with a simple single pulse of moment release. There appears to be a second pulse of moment release associated with this earthquake, visible as a shoulder on the source time functions in Figure 10. This could indicate a bilateral rupture, which would produce a rupture length of 80–120 km. A more likely interpretation is that the faulting process was more

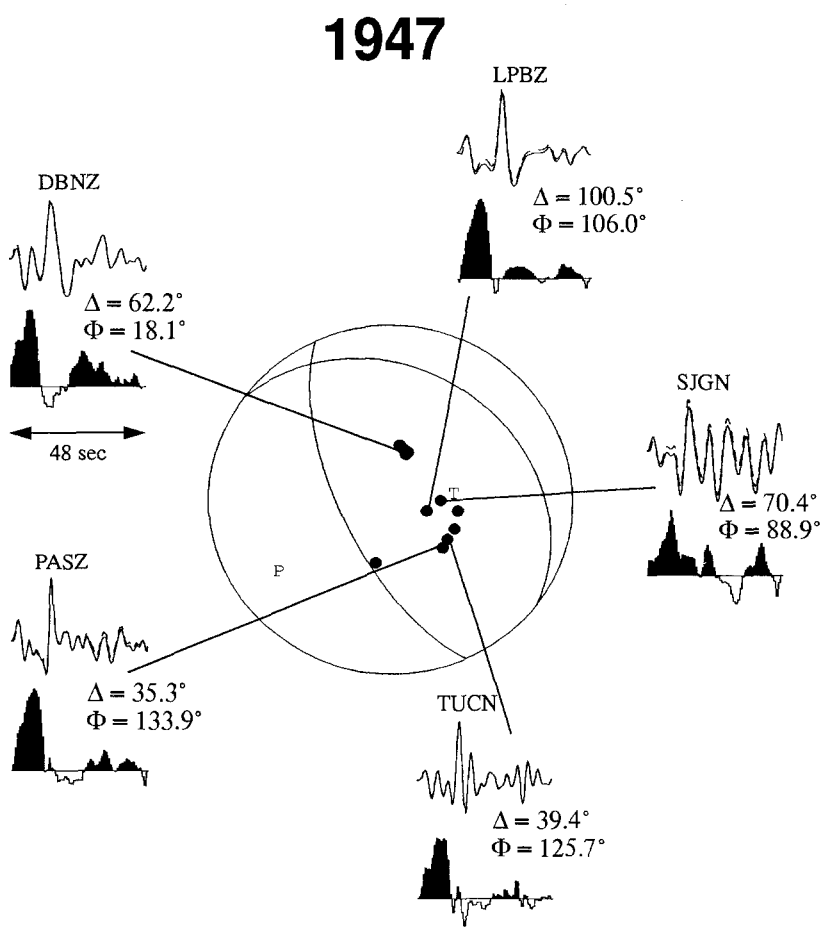

Figure 11
Focal mechanism of the 1947 earthquake used in the deconvolution, from WICKENS and HODGSON (1967). The first motions are from the ISS bulletins using only stations where polarities are verified. Deconvolved source time functions, using a distributed source Green's function, are shown for stations DBN, LPB, SJG, TUC and PAS. The data are shown by the solid traces, and the dashed traces are synthetics produced from the source time functions. Δ is the station-epicenter distance, and Φ is the station azimuth.

complicated than either a simple unilateral or bilateral mechanism. However, the calculated rupture lengths indicate that the whole of the SSZ may have ruptured in this event. The 1947 event, located to the south of the NE-SW trending Fairbanks seismic zone, was found to have a simple source time function with a duration of about 11 seconds, thus indicating a maximum unilateral rupture length of 33 km, applying the same assumptions as above. From these calculated rupture lengths and the depth, we can estimate the rupture area. Using this rupture area, along with the moment results, we can then go one step further and compute an average displace-

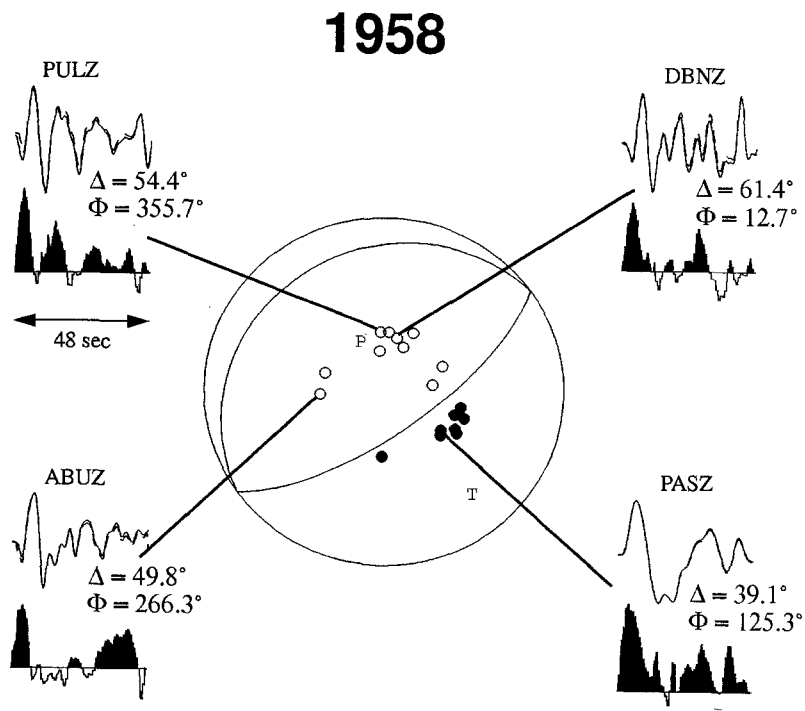

Figure 12
Focal mechanism of the 1958 earthquake used in the deconvolutions, from REISER (1990). The first motions are from the ISS bulletins, using only stations where polarities are verified. Deconvolved source time functions, using a distributed source Green's function, are shown for stations PUL, DBN, PAS, and ABU. The data are shown by the solid traces, and the dashed traces are synthetics produced from the source time functions. Δ is the station-epicenter distance, and Φ is the station azimuth.

ment for these events. We calculate a displacement of roughly three meters for the 1937 event and up to five meters for the 1947 event. No surface rupture was visible for either of these earthquakes, which is surprising given their size and depth.

The 1958 event is located between the Brooks Range to the north, and the right-lateral strike-slip Kaltag fault to the south. No known fault traces near the epicentral region have been identified despite a reconnaissance of the area shortly after the earthquake (DAVIS, 1960). However, the unconsolidated sand and alluvial deposits in the area perhaps conceal a fault in the competent rocks below. The most severe damage from the main shock occurred in a zone approximately 16 km wide by 64 km long trending northeast from Huslia, with the epicenter of the earthquake approximately in the center of this zone (DAVIS, 1960). The rupture duration of the 1958 earthquake, which occurred near Huslia, approximately 400 km ENE of Fairbanks, was found to be about 9 seconds. If we assume a unilateral faulting mechanism, based on the single pulse of moment release visible in the source time functions for this event (Figure 12), and a reasonable rupture velocity, then we

obtain a rupture length consistent with the observed damage in this area. From the rupture length and depth we calculate a rupture area, from which we determine a rough estimate of the displacement to be two meters. The largest vertical displacement measured in the area was on a short NW trending fault, perpendicular to most fissures in the immediate area. The maximum upward movement of the northeast side of the fault was 1.4 meters. Another 35 measurements were taken on northeast striking fissures, lying parallel to the damage zone, indicating a net movement of the northwest side 1.15 meters downwards (DAVIS, 1960).

From the values for seismic moment that were calculated from the deconvolutions, we computed M_s using the following empirical relation, which assumes a stress drop of 50 bars (GELLER, 1976):

$$\log M_0 = 1.5M_s + 15.51 \quad \text{for } 6.76 < M_s < 8.12.$$

This gave values of $M_s = 7.5 \pm 0.3$, $M_s = 7.5 \pm 0.3$, and $M_s = 7.2 \pm 0.2$ for the 1937, 1947, and 1958 earthquakes, respectively. The reported values for M_s were 7.3, 7.2, and 7.3 for the three events, close to those calculated from the seismic moment determinations. Examining the felt areas of the earthquakes, we find the 1937 and 1947 earthquakes had a felt area similar in size and equal to approximately 800,000 km^2, whereas the 1958 earthquake had a reported felt area of less than 650,000 km^2 (BRAMHALL, 1938; ST. AMAND, 1948; DAVIS, 1960). Although the parameter of felt area is strongly related to population, this may indicate that the 1958 Huslia event produced a slightly smaller M_s than the 1937 or 1947 earthquakes, as our results suggest. Two $M_s > 6$ aftershocks occurred within a week of the 1958 event. While the reported locations of the two aftershocks are 40 km and 70 km away from the mainshock, the differences in travel times for the main shock and the aftershocks at over 70 stations indicate that the aftershocks cannot be located more than 30 km and 45 km from the main shock, which is more consistent with our calculated rupture length.

The study of historical earthquakes continues to be problematic. However, despite our sparse data set, we have obtained reliable information on the depth, rupture duration and seismic moment release of three historical earthquakes in central Alaska. We have also gained an insight into the nature of moment release associated with these large intraplate events.

Acknowledgments

This research has been supported by a grant from the USGS/NEHRP program 1434–92–G–2221. We thank Dominique Gillard for his assistance in using Martin Beisser's source parameter inversion code, and Stefan Wiemer for a critical review of the paper.

REFERENCES

ABE, K. (1981), *Magnitudes of Large Shallow Earthquakes from 1904–1980*, Phys. Earth Planet. Interiors *27*, 72–92.

ADKINS, J. N. (1939), *The Alaskan Earthquake of July 22, 1937*, Bull. Seismol. Soc. Am. *30*, 353–376.

BEAUDOIN, B. C., FUIS, G. S., MOONEY, W. D., NOKLEBERG, W. J., and CHRISTENSEN, N. I. (1992), *Thin Low-velocity Crust Beneath the Southern Yukon-Tanana Terrane, East Central Alaska: Results from Trans-Alaska Crustal Transect Refraction/Wide-angle Reflection Data*, J. Geophys. Res. *97*, 1921–1942.

BEISSER, M., and KIND, R. (1988), *The Reflectivity Method for SH-waves and for Different Structures at Source and Receiver Sites*, Geol. J. E*42*, 137–142.

BEISSER, M., WYSS, M., and KIND, R. (1990), *Inversion of Source Parameters for Subcrustal Earthquakes in the Hellenic Arc*, Geophys. J. Int. *103*, 439–450.

BEISSER, M. D., GILLARD, D., and WYSS, M. (1994), *Inversion for Source Parameters from Sparse Data Sets: Test of the Method and Application to the 1951 (M = 6.9) Kona, Hawaii, Earthquake*, J. Geophys. Res. *99*, 19661–19678.

BISWAS, N. N., AKI, K., PULPAN, H., and TYTGAT, G. (1986), *Characteristics of Regional Stresses in Alaska and Neighboring Areas*, Geophys. Res. Lett. *13*, 177–180.

BISWAS, N. N., and TYTGAT, G. (1988), *Intraplate Seismicity in Alaska*, Seismol. Res. Lett. *59*, 227–233.

BRAMHALL, E. H. (1938), *The Central Alaskan Earthquake of July 22 (1937)*, Bull. Seismol. Soc. Am. *28*, 71–75.

BROGAN, G. E., CLUFF, L. S., KORRINGA, M. K., and SLEMMONS, D. B. (1975), *Active Faults of Alaska*, Tectonophysics *29*, 73–85.

BRUESTLE, E., and MÜLLER, G. (1983), *Moment and Duration of Shallow Earthquakes from Love-wave Modelling for Regional Distances*, Phys. Earth Planet. Interiors *32*, 312–324.

CHRISTENSEN, D. H., and RUFF, L. J. (1985), *Analysis of the Trade-off between Hypocentral Depth and Source Time Function*, Bull. Seismol. Soc. Am. *75*, 1637–1656.

CLUFF, L. S., SLEMMONS, D. B., BROGAN, G. E., and KORRINGA, M. K. (1974), *Basis for Pipeline Design for Active-fault Crossings for the Trans-Alaska Pipeline System*, Houston, Texas, Alyeska Pipeline Service Company, 115.

DAVIES, J. N. (1983), *Seismicity of the Interior of Alaska—A Direct Result of Pacific-North American Plate Convergence?* (abstract), EOS *64*, 90.

DAVIS, T. N. (1960), *A Field Report on the Alaska Earthquakes of April 7, 1958*, Bull. Seismol. Soc. Am. *50*, 489–510.

DZIEWONSKI, A. M., and ANDERSON, D. L. (1981), *Preliminary Reference Earth Model*, Phys. Earth Planet. Interiors *25*, 297–356.

ESTABROOK, C. H., STONE, D. B., and DAVIES, J. N. (1988), *Seismotectonics of Northern Alaska*, J. Geophys. Res. *93*, 12026–12040.

ESTABROOK, C. H., and BOYD, T. M. (1992), *The Shumagin Islands, Alaska, Earthquake of 31 May 1917*, Bull. Seismol. Soc. Am. *82*, 755–774.

GEDNEY, L., and BERG, E. (1969), *The Fairbanks, Alaska Earthquakes of June 21, 1967; Aftershock Distribution, Focal Mechanisms and Crustal Parameters*, Bull. Seismol. Soc. Am. *59*, 73–100.

GEDNEY, L. D., ESTES, S., and BISWAS, N. (1980), *Earthquake Migration in the Fairbanks, Alaska Seismic Zone*, Bull. Seismol. Soc. Am. *70*, 223–241.

GEDNEY, L., and MARSHALL, D. (1981), *A Rare Earthquake Sequence in the Kobuk Trench, Northwestern Alaska*, Bull. Seismol. Soc. Am. *71*, 1587–1592.

GELLER, R. J. (1976), *Body Force Equivalents for Stress-drop Seismic Sources*, Bull. Seismol. Soc. Am. *66*, 1801–1804.

GRISCOM, A. (1976), *Aeromagnetic Map and the Interpretation of the Tanacross Quadrangle, Alaska*, U.S. Geological Survey Miscellaneous Field Studies Map MF-767A, scale 1:250,000, 2 sheets.

HODGSON, J. H., and MILNE, W. G. (1951), *Direction of Faulting in Certain Earthquakes of the North Pacific*, Bull. Seismol. Soc. Am. *41*, 221–242.

LAHR, J. C., PAGE, R. A., STEPHENS, C. D., and CHRISTENSEN, D. H. (1988), *Unusual Earthquakes in the Gulf of Alaska and Fragmentation of the Pacific Plate*, Geophys. Res. Lett. *15*, 1483–1486.

MACELWANE, J. B., and SOHON, F. W., *Introduction to Theoretical Seismology. Part II. Seismometry* (Wiley, New York 1932) 149 pp.

MÜLLER, G. (1985), *The Reflectivity Method: A Tutorial*, J. Geophys. *58*, 153–174.

NOKLEBERG, W. J., ALEINIKOFF, J. N., LANGE, I. M., SILVA, S. R., MIYAOKA, R. T., SCHWAB, C. E., and ZEHNER, R. E. (1992), *Preliminary Geologic Map of the Mount Hayes Quadrangle, Eastern Alaska Range, Alaska*, U.S. Geological Survey Open-File Report 92–594, scale 1:250,000, 39.

PAGE, R. A., PLAFKER, G., DAVIES, J. N., and PULPAN, H. (1989), *Block Rotation and Seismicity in East-central Alaska* (abstract), EOS *70*, 1337.

PAGE, R. A., BISWAS, N. N., LAHR, J. C., and PULPAN, H., *Seismicity of continental Alaska.* In *Neotectonics of North America* (eds. Slemmons, D. B., Engdahl, E. R., Zoback, M. D., and Blackwell, D.) (Geological Society of America, Decade Map Volume 1 1991) pp. 47–66.

PAGE, R. A., PLAFKER, G., and PULPAN, H. (1995), *Block Rotation in East-central Alaska: A Framework for Evaluating Earthquake Potential?* Geology *23*, 629–632.

PEWE, T. L., WAHRHAFTIG, C., and WEBER, F. (1966), *Geologic Map of the Fairbanks Quadrangle, Alaska*, U.S. Geological Survey Miscellaneous Geologic Investigations Map I–455, scale 1:250,000.

POPPE, B. B. (1979), *Historical Survey of U.S. Seismograph Stations*, U.S. Geological Survey Professional Paper 1906.

REISER, L. (1990), *A Source Mechanism for the 7 April 1958 Huslia, Alaska Earthquake*, Third Keck Research Symposium in Geology, Abstracts Volume.

RUFF, L., and KANAMORI, H. (1983), *The Rupture Process and Asperity Distribution of Three Great Earthquakes from Long-period Diffracted P Waves*, Phys. Earth Planet. Interiors *31*, 202–230.

SEIDL, D. (1980), *The Simulation Problem for Broad-band Seismograms*, J. Geophys. *48*, 84–93.

SIEH, K. E., *A review of geological evidence for recurrence times of large earthquakes.* In *Earthquake Prediction—An International Review* (eds. Simpson, D. W., and Richards, P. G.), Maurice Ewing Series, vol. 4 (American Geophysical Union, Washington, D.C. 1981) pp. 181–207.

ST. AMAND, P. (1948), *The Central Alaska Earthquake Swarm of October 1947*, Trans., AGU *29*, 613–623.

WICKENS, A. J., and HODGSON, J. H. (1967), *Computer Re-evaluation of Earthquake Mechanism Solutions, 1922–1962*, Dept. of Energy, Mines and Resources, Canada, Vol. XXXIII.

(Received January 6, 1995, revised June 5, 1995, accepted June 10, 1995)